HHS Public Access

Author manuscript

Exp Neurol. Author manuscript; available in PMC 2016 October 13.

Published in final edited form as:

Exp Neurol. 2016 September ; 283(Pt A): 16–28. doi:10.1016/j.expneurol.2016.05.025.

Primary blast injury causes cognitive impairments and hippocampal circuit alterations

Matthew Beamer[a,1], **Shanti R. Tummala**[a,1], **David Gullotti**[a], **Kathryn Kopil**[a], **Samuel Gorka**[a], **Ted Abel**[b], **Cameron R. "Dale" Bass**[f], **Barclay Morrison III**[g], **Akiva S. Cohen**[d,e], and **David F. Meaney**[a,c,*]

[a]Department of Bioengineering, University of Pennsylvania, Philadelphia, PA, USA

[b]Department of Biology, University of Pennsylvania, Philadelphia, PA, USA

[c]Department of Neurosurgery, University of Pennsylvania, Philadelphia, PA, USA

[d]Department of Anesthesiology and Critical Care Medicine, University of Pennsylvania, Philadelphia, PA, USA

[e]Division of Critical Care Medicine, Children's Hospital of Philadelphia, Philadelphia, PA, USA

[f]Department of Biomedical Engineering, Duke University, Durham, NC, USA

[g]Department of Biomedical Engineering, Columbia University, New York, NY, USA

Abstract

Blast-induced traumatic brain injury (bTBI) and its long term consequences are a major health concern among veterans. Despite recent work enhancing our knowledge about bTBI, very little is known about the contribution of the blast wave alone to the observed sequelae. Herein, we isolated its contribution in a mouse model by constraining the animals' heads during exposure to a shockwave (primary blast). Our results show that exposure to primary blast alone results in changes in hippocampus-dependent behaviors that correspond with electro-physiological changes in area CA1 and are accompanied by reactive gliosis. Specifically, five days after exposure, behavior in an open field and performance in a spatial object recognition (SOR) task were significantly different from sham. Network electrophysiology, also performed five days after injury, demonstrated a significant decrease in excitability and increase in inhibitory tone. Immunohistochemistry for GFAP and Iba1 performed ten days after injury showed a significant increase in staining. Interestingly, a threefold increase in the impulse of the primary blast wave did not exacerbate these measures. However, we observed a significant reduction in the contribution of the NMDA receptors to the field EPSP at the highest blast exposure level. Our results emphasize the need to account for the effects of primary blast loading when studying the sequelae of bTBI.

Keywords

Blast induced traumatic brain injury; Concussion; Blood-brain barrier

*Corresponding author at: Department of Bioengineering, University of Pennsylvania, 240 Skirkanich Hall, 210 South 33rd St., Philadelphia, PA 19104, USA. dmeaney@seas.upenn.edu (D.F. Meaney).

[1]These authors contributed equally to this manuscript.

1. Introduction

Often referred to as the signature injury of the Iraq and Afghanistan conflict, blast-induced traumatic brain injury (bTBI) in the military is a complex biomechanical process wherein the head is subjected to the blast wave (blast loading), possible acceleration from impact, and penetrating injuries from projectiles (DePalma, 2015; Rosenfeld et al., 2013). Although the epidemiology of traumatic brain injury (TBI) in the military population is now clearer (Center, 2012), there remains significant debate about whether the sequelae and underlying etiology of bTBI are distinct from those of non-blast TBI (Wall, 2012). A review of the existing literature shows conflicting reports with some studies finding no differences between the two modes of injury and others reporting that survivors of bTBI show a decline in self-rated health compared with those of non-blast TBI. Determining the differences between non-blast and blast TBI is difficult because the exact biomechanics of each injury is unknown (Heltemes et al., 2012).

Animal models of bTBI offer a direct method for evaluating the effect of primary blast exposure on the brain. In small animal models, either a shock tube or live explosives are most commonly used to deliver an idealized, Friedlander-type shock wave to the animal (Kovacs et al., 2014; Meaney et al., 2014; Nakagawa et al., 2008). It is increasingly recognized that shock tube studies also contain two phases of biomechanical loading to the brain – the blast load on the brain, and the additional head accelerations that occur from the wind forces behind the shockwave front (Dal Cengio Leonardi et al., 2012; Dal Cengio Leonardi et al., 2013; Sundaramurthy et al., 2012). These simultaneous injury mechanisms make the interpretation of shock tube studies difficult. For example, although some recent work suggests that primary blast loading causes no neurological impairment (Goldstein et al., 2012), other studies indicate that it does affect cognition (Budde et al., 2013; Heldt et al., 2014).

In this study, we assess the effects of primary blast loading on the murine brain. We used a system to expose only the head to blast loading, and introduced a method to minimize head accelerations that occur during this simulated blast event. Our results show that primary blast loading does not cause gross structural changes but causes changes in hippocampus-dependent behavior that are accompanied by reactive astrogliosis in the tissue and alterations in area CA1 circuitry. Our *in vivo* findings, coupled with our recent *in vitro* work (Effgen et al., 2014; Vogel et al., 2015), emphasize the need to define the unique mechanisms of primary blast, either isolated from or in combination with contact/acceleration injuries that contribute to outcome of TBI in the military environment.

2. Materials and methods

2.1. Blast exposure

All experiments were performed on adult male (12–16 weeks old) C57BL/6 mice (Charles River, Wilmington, MA). Animal care and use followed guidelines specified by the Institutional Animal Care and Use Committee of the University of Pennsylvania. A shock tube that provided controllable and reproducible input was used to simulate free-field blast

events (Alphonse et al., 2014). Animals were first deeply anesthetized with isoflurane (5% induction for 2 min; 2% maintenance for 3 min) and then placed in a holder positioned 1 cm outside the exit end of the shock tube (Fig. 1A). At this location the shock wave profile is not significantly different from that of the inside of the tube (Panzer et al., 2012), and there are minimal reflections of the shock wave into the tube, which results in a less complex loading profile across the surface of the head. A sorbothane-lined (Part 8514K51, McMaster-Carr, Princeton, NJ) aluminum casing protected the torso and extremities from the blast. Animals were oriented with their snouts facing the shock tube (Fig. 1A). Two different kinematic conditions were generated: 1) constrained motion, wherein head motion was constrained with a thin metal rod encircling the snout and a cervical collar positioned between the occiput and shoulders, and 2) unconstrained motion, wherein the head was allowed to move freely during blast loading. Sham animals were similarly positioned with their heads either constrained or unconstrained corresponding to the kinematic condition of injury. After blast or sham exposure, righting time (the time taken by an animal placed supine to roll onto its stomach) was used to assess neurological impairment.

2.2. Impulse levels

Animals were exposed to one of two blast levels (Fig. 1B, C) designed with past work as reference: 1) mild blast - peak incident overpressure of 215 ± 13 kPa, duration of 0.65 ± 0.04 ms, and an impulse of 46 ± 5 kPa * ms, which is within the range of conditions causing cognitive impairment in rodents following blast exposure (Kovacs et al., 2014), and 2) moderate blast - peak incident overpressure of 415 ± 41 kPa, duration of 1.04 ± 0.04 ms, and impulse of 148 ± 12 kPa * ms, which is above the threshold for changes in BBB permeability *in vitro* (Hue et al., 2013; Hue et al., 2015) and LTP deficits in organotypic slice cultures (Effgen et al., 2014; Vogel et al., 2015). This range of blast loading is comparable to exposure to a 105-mm artillery round at a standoff distance of 5–10 m. The effects of unconstrained motion were only examined at the lower exposure level, as the higher exposure resulted in significant mortality.

2.3. Blast loading biomechanics

Pressure transducers with sufficient dynamic frequency response (Endevco, model 8530B-200, San Juan Capistrano, CA) were used to record the pressure at the shock tube exit. An additional pressure transducer was placed adjacent to the torso to measure the overpressures experienced by the torso. An inline filter conditioning box (Alligator Technologies, USBPGF-S1, Costa Mesa, CA) with a 20-kHz cutoff frequency linear phase filter was used to avoid aliasing of the signal prior to data acquisition. To estimate head accelerations resulting from blast loading, a high-speed video acquisition system (Phantom v4.2 camera, Vision Research, Wayne, NJ) was used to record head motion during blast exposure. The resultant head velocities and accelerations were calculated as previously described (Gullotti et al., 2014).

2.4. Behavior assessment

Behavior was assessed over the first nine days following injury. Tests were ordered to minimize any intermixing effects among the different tests. A more complete description of these tests appears in a recent publication (Patel et al., 2014a). An automated software

program was used to analyze performance (http://www.seas.upenn.edu/~molneuro/autotyping.html). Briefly, the tests performed and the parameters used to assess neurological changes are listed below.

2.5. Elevated zero-maze

The time spent in the open and walled regions of an elevated zeromaze was used as a measure of anxiety-like behavior. These changes were measured one day after blast exposure.

2.6. Rotarod performance

A rotarod apparatus (model: ENV-577M, Med Associates Inc., Georgia, VT) that accelerated a rod linearly from 4 to 40 RPM over a five-minute session was used to assess motor coordination. The time lapsed until first fault (fault time) and the total time the animal remained on the rotating rod before falling (fall time) were recorded for each test. For animals that did not fault, fall time was used for fault. Three trials, separated by an hour each, were conducted on each of three consecutive days starting the day after blast exposure.

2.7. Open field test

Animals were left undisturbed in a 30 cm × 40 cm open field arena and videotaped with a ceiling-mounted camera for 30 min. The time spent by each animal in the outer periphery, center region and four corner quadrants was determined over five-minute intervals for the entire time period. Ambulation data was further categorized into exploring, walking, or sitting behavior. Open field changes were measured three days after blast exposure.

2.8. Spatial object recognition (SOR)

Mice were first acclimatized for ten minutes in an arena (30 cm × 40 cm) without objects and then in three ten-minute sessions to two distinct objects placed in the arena. Each session was separated by 1 h. Twenty-four hours later, one of the objects was displaced and mice were recorded for a fifth ten-minute session. The amounts of time the animal spent interacting with the objects and exploring the remainder of the field were quantified. The animal's preference for the displaced object over the non-displaced object in the fifth session was measured. The SOR paradigm was implemented on days 4 and 5 following blast exposure.

2.9. Fear conditioning

Contextual fear conditioning was performed as described previously (Patel et al., 2014a). On the first day of the testing sequence, the animal was placed in a conditioning chamber (Coulbourn Instruments, Whitehall, PA) for 2 min and twenty-eight seconds before the onset of a foot shock (2-s, 1.5 mA). Contextual conditioning was assessed 24 h later by placing the animal back in the same chamber for 5 min. The animal's trajectory during this period was analyzed to identify periods of freezing behavior. The percent of time spent in a freezing posture was used as a measure of the conditioned fear response. The fear conditioning paradigm was implemented on days 8 and 9 following blast exposure.

2.10. Acute hippocampal slice preparation and recording

Animals were decapitated under isoflurane anesthesia and their brains were quickly isolated into ice-cold, oxygenated (95% O_2, 5% CO_2) sucrose-based artificial cerebrospinal fluid (ACSF) consisting of (in mM) 202 sucrose, 3 KCl, 2.5 NaH_2PO_4, 26 $NaHCO_3$, 10 glucose, 1 $MgCl_2$ and 2 $CaCl_2$. Coronal sections (350 μm thick) were cut using a vibratome (VT1200S, Leica Microsystems, Buffalo Grove, IL), transferred to oxygenated ACSF (comprising, in mM, of 130 NaCl, 3 KCl, 1.25 NaH_2PO_4, 26 $NaHCO_3$,10glucose, 1$MgCl_2$, and 2 $CaCl_2$),and maintained at 34–36 °C. Prior to recording, slices were transferred to room temperature (22–24 °C) in an interface chamber perfused with oxygenated ACSF (2–4 ml min^{-1}).

Field potentials were recorded in the CA1 region of the dorsal hippocampus (1.58–2.30 mm posterior to Bregma) from either hemisphere by an Axoclamp 900 A amplifier interfaced with pClamp 10 data acquisition software (Molecular Devices, Sunnyvale, CA, USA). The stimulating electrode (#CBDPG75, Frederick Haer Corporation, Bowdoin, ME) was placed in the stratum radiatum (SR) at the boundary between the CA1 and CA2 regions, approximately two thirds of the length of the SR from the cell body layer (stratum pyramidale; SP). The recording electrode was similarly placed in the SR in CA1 at approximately two thirds of the length of the SR from the SP and 700–1100 μm from the stimulating electrode (Johnson et al., 2014). For population spike responses, the recording electrode was placed adjacent to the stratum pyramidale and stratum oriens layers at a similar distance from the recording electrode. Both electrodes were gradually positioned at a depth at which the maximum amplitude of the measured parameter (slope of the linear portion of the response in SR and the amplitude of the population spike in SP) was obtained. Recording electrodes were fabricated from borosilicate glass capillaries (#1B150F-4, World Precision Instruments, Sarasota, FL) to have a tip resistance of 2–6 MΩ and filled with ACSF. The electrical stimulus was 100 μs in duration, and was biphasic, with the negative phase appearing first. Recorded signals were low-pass filtered at 2 kHz.

Field potentials were recorded five days after treatment (shamor injury). Input-output (I/O) curves were first obtained for all slices for stimulus intensities in the range of 40–400 μA. The stimuli were incremented by 40 μA, and were 8 s apart. The stimulation pattern was repeated three times and the slopes of the three repetitions were averaged. The stimulus intensity at which the half-maximum slope was obtained was used to examine release probability using paired-pulses. The pair of stimuli was delivered 25, 50, 75 and 100 milliseconds apart. For each inter-stimulus interval, the measured slopes in three trials (separated by 8 s) were averaged and the ratio of the second to the first slope was calculated.

Contribution of the NMDA receptors to the field potential was isolated through perfusion of 6 μM CNQX (Abcam, Cambridge, MA) in reduced magnesium ACSF (mACSF) comprising of (in mM): 130 NaCl, 3 KCl, 1.25 NaH_2PO_4, 26 $NaHCO_3$, 10 glucose, 0.5 $MgCl_2$, and 2 $CaCl_2$. The stimulus intensity for half-maximum slope was used to determine the baseline during drug perfusion. The stimulus was delivered every 30s until the decreasing slope stabilized at its final value (typically 20– 30 min). Input-output (I/O) curves were determined as described above. Relative contribution of the inhibitory neurons to the field

potential was tested in a different set of slices by measuring field I/O curves in the presence of bicuculline methiodide (BMI; 30 μM; Abcam, Cambridge, MA) added to ACSF.

2.11. Histology and immunohistochemistry

Ten days following blast exposure, animals were anesthetized with an overdose of sodium pentobarbital and transcardially perfused with 20 ml of ice-cold PBS (1×;pH7.4) followed by 40 ml of freshly prepared ice-cold 4% paraformaldehyde. Brains were isolated, fixed overnight in 4% paraformaldehyde at 4 °C and cryoprotected in 24% sucrose phosphate buffer (pH 7.4). Perfused brains were then embedded in paraffin and cryosectioned into 20 μm sections. Sections were evenly distributed over five replicate series, with a spacing of 200 μm between sections within a series. Prior to staining, sections were successively rinsed with xylene (2 × 5 min); ethanol 100% (2 × 1 min), 95% (1 min), 80% (1 min) and 70% (1 min); and distilled water. For immunohistochemistry, sections were then immersed for 30 min in a mixture of methanol and hydrogen peroxide (5:1), washed for 10 min in running water and blocked for 5 min with 2% fetal bovine serum in 0.1 M Tris buffer (pH 7.6). Sections were soaked in primary antibody overnight at 4 °C. The primary antibodies used were rabbit anti-GFAP (1:20000; Abcam, Cambridge, MA) and rabbit anti-Iba1 (1:1000; Wako, Richmond, VA). For Iba1 staining, antigen retrieval was performed prior to treatment with the methanol–hydrogen-peroxide mixture by immersing the sections in 88% formic acid for 5 min and rinsing with distilled water for 5 min. The primary antibody was rinsed with 0.1 M Tris buffer and sections were soaked in the secondary antibody (affinity purified biotinylated anti-rabbit IgG, Vector Laboratories, CA) for 1 h at room temperature. Sections were then rinsed (0.1 M Tris buffer), soaked in ABC solution (Vectastain kit, Vector Laboratories, Inc., Burlingame, CA) for 1 h at room temperature, rinsed (0.1 M Tris buffer), immersed in DAB (Vector Laboratories, Inc., Burlingame, CA) for 1.5–5 min, and cover slipped. For cresyl violet (FD Neurotechnologies, Inc., Columbia, MD) and hematoxylin and eosin staining, sections were soaked in cresyl violet solution (0.1% for 35 min) or Shandon Harris hematoxylin (ThermoScientific, Waltham, MA; 5 min) subsequent to rinses with xylene and varying concentrations of ethanol, and rinsed with distilled water. Sections exposed to cresyl violet were then treated with a mixture (1000:1; for 30 s) of 95% ethanol and 0.1% glacial acetic acid, followed by 100% ethanol (for 1 min) and xylene (2 × 5 min), and cover slipped. Sections exposed to hematoxylin were treated with a mixture of hydrochloric acid (0.1%) and ethanol (50%) for 2 s, washed in running water for 15 min, treated with eosin for 45 s, rinsed successively with distilled water, 95% (1 min), 100% ethanol (1 min) and xylene (2 × 5 min), and cover slipped.

Sections from corresponding sham and injured animals were processed and imaged simultaneously. Low magnification images were acquired with a light microscope (Leica DM4000 B, Leica Microsystems, Buffalo Grove, IL) fitted with a camera (Leica DFC340FX) with a 5× objective. Higher magnification images were acquired with a confocal scanning laser microscope (Leica TCS SP5, Leica Microsystems, Buffalo Grove, IL) with 40× or 63× objectives. Images from all the three groups, for any given staining, were acquired under identical acquisition parameters and settings. Intensity of immunohistochemical staining was quantified using ImageJ. Briefly, regions of interest were drawn around the brain structure or tissue of interest, and the area of staining was measured

using the analyze particles function based on an intensity threshold. The image processing parameters were identical across all the groups.

2.12. Statistical analysis

Statistical differences in behavior and histological staining among the different experimental groups (sham, constrained motion (both levels), unconstrained motion) were assessed using one-way ANOVA or repeated measures (RM) ANOVA as appropriate. When significant, post-hoc comparisons were done with Tukey's test. The Shapiro-Wilk test was used to determine normality and nonparametric versions of the tests (Kruskal-Wallis and Mann-Whitney U) were employed as needed. Comparison of the field electrophysiology data (I/O curves, population spike and paired pulse facilitation) between the two blast loading levels and sham was done using a generalized linear model wherein the variability between slices and animals in each group was accounted for in the analysis. For the pharmacology data, a paired *t*-test was used to determine the effect of the applied drug on a slice within a group. The effect of a drug on slices in two groups was compared using a Student's *t*-test and in three groups with one-way ANOVA. A *p*-value less than or equal to 0.05 was considered significant. All values are reported as mean ± s.e.m. unless otherwise noted.

3. Results

3.1. Constraining the snout and shoulders significantly decreases head acceleration

Recent work shows that blast loading using a shock tube can result in significant acceleration of the head (Gullotti et al., 2014). Consequently, to isolate the effects of primary blast loading on the brain, we devised a strategy to constrain the head from moving and first evaluated its efficacy. Similar to previous work (Sundaramurthy et al., 2012), we found that head accelerations are significant when the head is not constrained ($22.54 \pm 10.03 \times 10^3$ m s^{-2}, $n = 13$) during blast loading (Fig. 1F). However, constraining both the snout and shoulders (Fig. 1A, D, E) significantly reduced head accelerations ($3.4 \pm 1.12 \times 10^3$ m s^{-2}, $n = 8$; $p < 0.0001$ relative to unconstrained, Student's *t*-test). Furthermore, there was no significant difference in accelerations for the constrained configuration when animals were exposed to either mild ($3.4 \pm 1.12 \times 10^3$ m s^{-2}, $n = 8$) or moderate ($3.25 \pm 1.4 \times 10^3$ m s^{-2}, $n = 5$; $p = 0.97$, Student's *t*-test; Fig. 1G) blast loading.

3.2. Blast exposure causes behavioral changes that are compounded when the head is allowed to move freely

We first tested whether cognitive deficits were affected by constraining the head during blast exposure (Fig. 2). We found no significant differences in any of the behavioral measures between the constrained and unconstrained sham animals; the two sham groups were therefore combined into a single sham group ($n = 21$). Righting time (Fig. 2B) was significantly longer in the unconstrained ($n = 13$) group relative to the sham and constrained ($n = 21$) groups ($p < 0.001$; one-way ANOVA; Tukey's post-hoc). Some measures of behavior, e.g., the time to first exit (Fig. 2C) the walled portions of an elevated zero-maze ($p = 0.16$, Kruskal-Wallis) were not significantly different among the three groups, indicating that the mechanisms underlying these behaviors were unaffected by blast loading. In contrast, both the head constrained and unconstrained animals showed a lower preference for

the displaced object compared with the sham animals ($p = 0.01$, one-way ANOVA, Tukey's post-hoc; Fig. 2D). Fear conditioning, measured nine days after blast exposure, was reduced in the unconstrained animals relative to sham animals, but this difference was not significant ($p = 0.05$, Kruskal-Wallis; Fig. 2E). This difference was no longer evident once the head was constrained.

3.3. Behavioral changes resulting from constrained blast loading are similar across exposure levels

Given that blast loading resulted in some behavioral differences when the head was constrained from moving, we next tested if these differences were exacerbated with increased blast impulse exposure levels. Righting time increased significantly at the higher blast level relative to sham and the lower blast overpressure level ($p < 0.001$, one way ANOVA, Tukey's; Fig. 3B). We observed no effect of blast overpressure loading on the time to first exit ($p = 0.86$; one-way ANOVA) or time in the open region of the elevated zero-maze test ($p > 0.90$; oneway ANOVA, Fig. 3C) relative to sham. Similarly, we observed no difference in rotarod performance over any of the individual testing days among the groups (Fig. 3D; $p = 0.34$). However, injured animals spent significantly less time in the center of an open field for both blast levels (Fig. 3E; $p < 0.05$, one-way ANOVA, Tukey's posthoc), were less ambulatory (i.e., walked and explored) for the lower blast exposure level ($p < 0.01$, one-way ANOVA, Tukey's posthoc; Fig. 3E), and exhibited pronounced thigmotaxis (wall-hugging) behavior (Fig. 3F) for both exposure levels compared with sham ($p = 0.04$, one-way ANOVA, Tukey's pothoc). Interestingly, we did not observe a significant difference in the time spent within the center region, in total distance traversed (ambulation), and in thigmotaxis between the low and high exposure levels (Figs. 3E, F). Both groups of injured animals displayed a significantly decreased preference for the displaced object compared with sham ($p = 0.02$, one-way ANOVA, Tukey's posthoc; Fig. 3G). Although there was a reduction in the percent freeze time in fear conditioning at the highest level, we did not observe a significant difference across blast and sham exposures ($p = 0.54$, one-way ANOVA; Fig. 3H). Together, these findings show that primary blast exposure causes similar behavioral impairments across two distinct blast exposure levels i.e., mild and moderate.

3.4. Constrained blast loading results in gliosis with minimal changes tobrain structure

The behavioral changes observed following primary blast loading suggest that either the morphology or circuitry was altered by the transmitting shockwave. Consequently, we first determined if there was any structural damage to the brain. We found no changes in the gross morphology of both mild and moderate blast exposed brains compared with sham. Staining with both cresyl violet or hematoxylin and eosin showed no areas with neuronal atrophy, hypertrophy, or generalized loss of neuronal density 10 days after blast exposure at either level (Fig. 4A and B show staining in the hippocampus). Given this lack of overt damage to neuronal architecture, we explored possible changes in glial reactivity. Immunohistochemistry showed enhanced labeling for GFAP in the hippocampus at both exposure levels (Fig. 5A, C; $p = 0.01$, Kruskal-Wallis, Dunn's test). Similarly, the intensity of Iba1 staining, indicative of reactive microglia, was higher throughout the hippocampi (Fig. 5B, D) of injured animals compared with sham ($p < 0.01$, Kruskal-Wallis, Dunn's test). However, similar to the observations in open field and SOR behavior, there were no

significant differences in staining intensities between the two levels of injury in the hippocampus.

3.5. Excitability of hippocampal area CA1 is reduced and inhibitory tone is increased subsequent to constrained blast loading

With no apparent changes in neuronal density but a significant increase in reactive gliosis, we next determined if the behavioral changes corresponded with alterations in hippocampal circuitry. Extracellular field excitatory postsynaptic potentials (fEPSP) recorded in the SR (stratum radiatum) of blast-exposed animals (Fig. 6A, B) showed a significant reduction in slope subsequent to both mild and moderate blast exposure relative to sham ($p < 0.01$ across all stimulation levels, generalized linear model, Wald test). Similar to the behavior and immunohistochemistry results, there was no significant difference in the field I/O (input-output) curves between the two blast exposure levels (Fig. 6B). Given the decrease in the fEPSP response, we examined if this was due to altered probability of release from the presynaptic terminals. We determined this using a paired pulse protocol (Fig. 6D). Similar to recent *in vitro* work (Vogel et al., 2015), there were no significant differences in paired pulse facilitation between the three groups ($p = 0.21$, generalized linear model), indicating that the decrease in fEPSP responses may not be due to altered probability of release from the presynaptic terminals.

Recent *in vitro* work in our laboratory showed that the contribution and composition of the NMDA receptors are altered following stretch injury (Patel et al., 2014b), and we asked if a similar phenomenon occurred after primary blast loading. We therefore tested if the relative contribution of the NMDA receptors to the field potential was affected after primary blast loading (Fig. 6A, C). Interestingly, exposure to the higher impulse resulted in a significant decrease in the contribution of the NMDA receptor to the field potential compared with that of the sham group ($p < 0.029$ for all intensities except 40 μA, One-way ANOVA, Tukey's post-hoc). Though not significantly different from the higher blast group at any intensity and the sham group beyond 200 μA, the contribution of the NMDA receptor following mild blast exposure is intermediate between that of the sham and moderate blast groups. Most interestingly, this indicates that increasing the impulse results in subtle alterations to the receptor composition and dynamics.

Given the decrease in net synaptic efficacy in area CA1 neurons (as suggested by the SR field responses), we next asked if the output was similarly reduced. An indirect measure of output is the field population spike recorded in SP (stratum pyramidale; Fig. 6E). There was no significant change in the population spike amplitudes subsequent to moderate blast loading at any intensity and after mild blast loading up to 280 μA ($p > 0.05$ for all intensities except 320–400 μA, generalized linear model). Reduced network excitability in area CA1 after brain injury has also been observed in models of non-blast TBI and was shown to be due to a shift towards inhibition in the excitatory-inhibitory tone (Cole et al., 2010; Witgen et al., 2005). To test if the same phenomenon was occurring subsequent to primary blast loading, we bath applied BMI in ACSF to a subset of slices from the higher impulse group after acquiring field I/O curves. In sham slices, treatment with BMI modestly increased the field I/O curve at the higher intensities ($p < 0.03$, 200–400 μA, paired *t*-test; Fig. 6F).

Without BMI treatment, the field I/O curves from injured animals were significantly smaller relative to sham animals (Fig. 6G). Treatment with BMI significantly reversed the reduction in field I/O curves collected from blast-injured animals (pre vs. post, $p < 0.01$ for all intensities, paired *t*-test; Fig. 6G); the treated, injured group was no longer significantly different from either the treated sham group ($p > 0.10$, Student's *t*-test) or the untreated sham group ($p > 0.05$, Student's *t*-test). Together, these data suggest that inhibition may be augmented in CA1 circuitry following blast exposure, similar to results reported by Witgen et al. (2005) and Johnson et al. (2014).

4. Discussion

Although the prevalence of bTBI in the military is now more fully described (Hoge et al., 2008; Schwab et al., 2007; Terrio et al., 2009), there remains uncertainty on which phase of the mechanical loading – the primary blast wave transmitting through the brain, the secondary impact/acceleration that occurs in some situations, and potential penetrating injury – causes the sequelae that are commonly observed in bTBI survivors. Our main aim was to compare the behavioral changes that appear following closed-head blast exposure in conditions where the head is allowed to freely accelerate in response to the overpressure loading, relative to the changes that appear following a second condition where head motion is restricted. We found that both experimental conditions led to significant behavioral impairments, with some deficits persisting when head acceleration was minimized during blast. In addition, we found significant deficits in hippocampal network excitability and increases in glial reactivity even when the head was restrained during blast. Together, these data show that blast overpressure loading, even when head motion is minimized, is capable of creating measurable structural, functional, and behavioral alterations in the brain.

In human blast TBI, several recent studies report alterations in hippocampal volume, differences in slow wave generation measured with magnetoelectroencephalography, and biochemical changes detected with magnetic resonance spectroscopy within regions that include the hippocampus (de Lanerolle et al., 2014; Huang et al., 2014). Preclinical rodent studies show blast exposure will cause alterations in hippocampal microstructure, increases in different forms of phosphorylated Tau, reductions in axonal conduction velocity, and LTP deficits in the hippocampal circuitry after injury (Budde et al., 2013; Effgen et al., 2015; Goldstein et al., 2012; Huber et al., 2013; Vogel et al., 2015; Yin et al., 2014). We demonstrate that despite no clear sign of neuronal loss, blast exposure will reduce hippocampal network excitability in area CA1, and that these changes do not differ across these two blast exposure levels. Although some past work shows no reduction in excitability after blast exposure (Goldstein et al., 2012), our findings are more consistent with work by Rasband and colleagues that demonstrated that a blast exposure in rats led to a reduction in hippocampal excitability (Baalman et al., 2013). A few reasons may contribute to the differences we observe with previous work (Goldstein et al., 2012). Perhaps the most significant reason is that the magnitude and direction of the blast wave differs between studies, and therefore the transmission of the blast wave through the brain could alter the local deformations that appear within the hippocampal circuitry, subsequently affecting impairment. Relatedly, the impulse of the loading in our current study is higher than the conditions used in the Goldstein study, which may also explain the relative increase in

impairment that we observed after blast exposure. A final reason may be methodological, as our observed field I/O deficits are apparent only at higher stimulation levels when the response plateaus, while Goldstein and colleagues focused on lower stimulation levels (below 100 μA) when responses in both injured and sham groups are small and not different from each other.

At our highest blast pressure level, we also saw a shift in the relative contribution of NMDA receptors to the field I/O curves, indicating that blast overpressure is capable of altering functional synaptic characteristics similar to other experimental TBI models (Howard et al., 2007; Santhakumar et al., 2000; Yang et al., 2007). Our observation that pharmacologically blocking $GABA_A$ neurotransmission will reverse the blast-induced deficits in field I/O curves indicates that the inhibitory network may be the key mediator of hippocampal impairment, similar in nature to the role that inhibitory neurons play in some prior studies of experimental TBI (Bonislawski et al., 2007; Ding et al., 2011; Hunt et al., 2011; Johnson et al., 2014; Johnstone et al., 2013; Schwarzbach et al., 2006). In the longer term, these findings point towards GABAergic signaling as a potential therapeutic target in TBI.

Our observation that primary blast exposure causes broad changes in glial reactivity with no significant evidence of neuronal loss or degeneration is consistent with some past rodent (Svetlov et al., 2010) and porcine models of bTBI (Bauman et al., 2009; de Lanerolle et al., 2011), and some aspects of past in vitro work (Effgen et al., 2014; Effgen et al., 2015; Vogel et al., 2015). Similar to our data on hippocampal circuit alterations, we did not observe a significant dose response in glial reactivity between the lower- and higher-level blast overpressure loading. However, one mechanism speculated to increase glial reactivity is the disruption of the blood-brain barrier (BBB) in areas of mechanical stress concentration (Bandak et al., 2015). Breakdown of the BBB after blast exposure is commonly reported (Elder et al., 2015; Kabu et al., 2015; Readnower et al., 2010; Shetty et al., 2014; Yeoh et al., 2013). We recently found significant changes in BBB integrity following primary blast loading *in vitro* and *in vivo* (Hue et al., 2014; Hue et al., 2013; Hue et al., 2015). Unlike the *in vitro* preparations, even a very small compromise of the blood-brain barrier could lead to serum components leaking into the extracellular space and triggering a strong gliotic response. As such, it is not surprising that there is a somewhat smaller impulse needed for causing gliosis after blast overpressure *in vivo versus* the conditions necessary for *in vitro* compromise. However, the implication of increased reactivity on circuit function is less clear. Increased glial reactivity was previously shown to increase excitability in CA1 (Ortinski et al.,2010). However, we observed a decrease in network excitability in this work, suggesting that increased glial reactivity is not the sole cause for alterations in the hippocampal circuitry after primary blast loading. Our results suggest instead that alterations in synaptic components and thresholds for circuit activity, in combination with increased glial reactivity, contribute to the observed hippocampal pathology.

We purposefully examined a broad range of behavioral tasks, given that very little is known on the extent and type of damage that appears throughout the brain after blast exposure. This approach is different from past work that often focused on one type of behavioral deficit, whether it was related to anxiety (Patel et al., 2014a; Xie et al., 2013; Yin et al., 2014), memory (Ning et al., 2013; Rubovitch et al., 2011), or motor impairment (del Mar et al.,

2015). With our interest in primary blast loading, we focused on understanding a deficit in spatial object recognition that remained even when the head was restrained during blast exposure. Although SOR impairment did not occur with any overt sign of neuronal loss in the hippocampus, it did occur with significant impairment in field I/O curves from the CA1. We were somewhat surprised that the impairment in spatial object recognition did not worsen with increasing blast severity, though, and additional studies to explore how this impairment is affected by the direction and complexity of the blast wave is warranted. These additional studies may also resolve past work that shows blast exposure can differentially affect hippocampal-dependent behaviors (Budde et al., 2013; Sajja et al., 2015; Tompkins et al., 2013; Tweedie et al., 2013), a discrepancy that can be explained by characteristics of the blast loading.

From a biomechanical standpoint, these data confirm that primary blast can cause both behavioral and hippocampal circuit impairments. A previous study showed that eliminating head motion during blast eliminates any behavioral impairment (Goldstein et al., 2012), leading to a growing perception that blast-induced acceleration is required to cause damage in bTBI. This perception is further complicated by field data that shows that approximately 80% of TBI in the military occurs in the non-deployed setting (http://dvbic.dcoe.mil/dod-worldwide-numbers-tbi), indicating that primary blast is less common than other injury mechanisms. However, Tate et al. (Tate et al., 2013) showed that breachers who experience blast without blunt impact still exhibit neurological changes and changes in serum biomarkers. Drawing a direct connection from this human volunteer study to our work, though, is not easy because these human volunteers were involved in multiple exposures and we only examined a single blast exposure. Moreover, past work from our group shows that blast overpressure *in vitro* will cause reductions in the hippocampal circuit activity and a loss in synaptic plasticity (Effgen et al., 2014; Effgen et al., 2015; Vogel et al., 2015). Surprisingly, our data show very little dose response effect in the behavioral deficits that occur when the blast exposure is nearly doubled in magnitude. These data point towards a critical need to first establish the minimal exposure dose, rather than the dose response, for behavioral deficits that can occur following blast overpressure loading. In the long term, we envision linking blast loading metrics with bTBI risk probabilities, similar in nature to the approach used for acceleration-based measures from field studies in American football (Rowson and Duma, 2013).

Extending our current work to develop thresholds for human blast exposure would require careful consideration of how to scale the blast exposures used in rodent studies. We are aware of the current limitations for proposed scaling relationships of blast overpressure loading to the brain, and used available scaling guidelines (Bass et al., 2012; Jean et al., 2014; Rafaels et al., 2011) to adjust both the pressure and duration of the blast input to mimic a free field exposure that resembled a charge of 105 mm artillery round with a standoff distance of 5–10 m. Rodent studies of blast exposure to date rarely considered scaling the blast overpressure waveform and frequently reported only specific loading parameters. For example, it is quite common to see the peak overpressure reported, but far less common to see the duration and impulse reported (Panzer et al., 2014; Sundaramurthy et al., 2012). For other regions of the body, a more complete description of the loading condition eventually led to scaling laws that allowed one to transfer these from the

laboratory to the scenario in theater and *vice versa*, and helped develop protective equipment (Bass et al., 2008; Bowen et al., 1968). To date, there is no such consensus on how to report experimental blast conditions for models of bTBI, although there is now an agreement for developing common preclinical data elements in TBI models (Smith et al., 2015) and these more extensive loading conditions should be considered part of the archived information. In addition to the parameters of loading these should include both the direction of the propagating wave, orientation of the head, and possible reloading from multiple reflections of the shockwave. Nevertheless, our data, in combination with other past studies, provides more clarity and support to the principle that blast overpressure can affect structure, circuits, and behavior.

To summarize, it is evident that we are only at the beginning of understanding the causal factors in and tolerance of the brain to blast loading. Although a growing consistency across many laboratories indicates that the histological damages in mild TBI from blast exposure include glial reactivity, minimal to no neuronal loss, and some evidence of axonal damage, we are not yet clear on how these changes translate to circuit and behavioral impairments. Our work confirms that these changes can occur from the primary phase of the blast wave, and emphasizes the need to better understand the mechanistic similarities and differences that occur between this type of loading and other mechanical loading inputs that can cause damage to the brain.

Acknowledgments

The authors thank Dr. Brian N. Johnson for his help and assistance over the course of this study. Funding was provided by the Army Research Office through W911NF-10-1-0526.

References

Alphonse VD, Siva Sai Sujith Sajja V, Kemper AR, Rizel DV, Duma SM, VandeVord PJ. Membrane characteristics for biological blast overpressure testing using blast simulators. Biomed Sci Instrum. 2014; 50:248–253. [PubMed: 25405432]

Baalman KL, Cotton RJ, Rasband SN, Rasband MN. Blast wave exposure impairs memory and decreases axon initial segment length. J Neurotrauma. 2013; 30:741–751. [PubMed: 23025758]

Bandak FA, Ling G, Bandak A, De Lanerolle NC. Injury biomechanics, neuropathology, and simplified physics of explosive blast and impact mild traumatic brain injury. Handb Clin Neurol. 2015; 127:89–104. [PubMed: 25702211]

Bass CR, Rafaels KA, Salzar RS. Pulmonary injury risk assessment for short-duration blasts. J Trauma. 2008; 65:604–615. [PubMed: 18784574]

Bass CR, Panzer MB, Rafaels KA, Wood G, Shridharani J, Capehart B. Brain injuries from blast. Ann Biomed Eng. 2012; 40:185–202. [PubMed: 22012085]

Bauman RA, Ling G, Tong L, Januszkiewicz A, Agoston D, Delanerolle N, Kim Y, Ritzel D, Bell R, Ecklund J, Armonda R, Bandak F, Parks S. An introductory characterization of a combat-casualty-care relevant swine model of closed head injury resulting from exposure to explosive blast. J Neurotrauma. 2009; 26:841–860. [PubMed: 19215189]

Bonislawski DP, Schwarzbach EP, Cohen AS. Brain injury impairs dentate gyrus inhibitory efficacy. Neurobiol Dis. 2007; 25:163–169. [PubMed: 17045484]

Bowen IG, Fletcher ER, Richmond DR, Hirsch FG, White CS. Biophysical mechanisms and scaling procedures applicable in assessing responses of the thorax energized by air-blast overpressures or by nonpenetrating missiles. Ann N Y Acad Sci. 1968; 152:122–146. [PubMed: 5257525]

Budde MD, Shah A, McCrea M, Cullinan WE, Pintar FA, Stemper BD. Primary blast traumatic brain injury in the rat: relating diffusion tensor imaging and behavior. Front Neurol. 2013; 4:154. [PubMed: 24133481]

Center, D.a.V.B.I. DoD Worldwide Numbers for TBI. 2012

Cole JT, Mitala CM, Kundu S, Verma A, Elkind JA, Nissim I, Cohen AS. Dietary branched chain amino acids ameliorate injury-induced cognitive impairment. Proc Natl Acad Sci U S A. 2010; 107:366–371. [PubMed: 19995960]

Dal Cengio Leonardi A, Keane NJ, Bir CA, Ryan AG, Xu L, Vandevord PJ. Head orientation affects the intracranial pressure response resulting from shock wave loading in the rat. J Biomech. 2012; 45:2595–2602. [PubMed: 22947434]

Dal Cengio Leonardi A, Keane NJ, Hay K, Ryan AG, Bir CA, VandeVord PJ. Methodology and evaluation of intracranial pressure response in rats exposed to complex shock waves. Ann Biomed Eng. 2013; 41:2488–2500. [PubMed: 23904049]

de Lanerolle NC, Bandak F, Kang D, Li AY, Du F, Swauger P, Parks S, Ling G, Kim JH. Characteristics of an explosive blast-induced brain injury in an experimental model. J Neuropathol Exp Neurol. 2011; 70:1046–1057. [PubMed: 22002430]

de Lanerolle NC, Hamid H, Kulas J, Pan JW, Czlapinski R, Rinaldi A, Ling G, Bandak FA, Hetherington HP. Concussive brain injury from explosive blast. Ann Clin Transl Neurol. 2014; 1:692–702. [PubMed: 25493283]

del Mar N, von Buttlar X, Yu AS, Guley NH, Reiner A, Honig MG. A novel closed-body model of spinal cord injury caused by high-pressure air blasts produces extensive axonal injury and motor impairments. Exp Neurol. 2015; 271:53–71. [PubMed: 25957630]

DePalma, RG. Combat TBI: history, epidemiology, and injury modes. In: Kobeissy, FH., editor. Brain Neurotrauma: Molecular, Neuropsychological, and Rehabilitation Aspects. Boca Raton (FL): 2015.

Ding MC, Wang Q, Lo EH, Stanley GB. Cortical excitation and inhibition following focal traumatic brain injury. J Neurosci. 2011; 31:14085–14094. [PubMed: 21976493]

Effgen GB, Vogel EW 3rd, Lynch KA, Lobel A, Hue CD, Meaney DF, Bass CR, Morrison B 3rd. Isolated primary blast alters neuronal function with minimal cell death in organotypic hippocampal slice cultures. J Neurotrauma. 2014; 31:1202–1210. [PubMed: 24558968]

Effgen GB, Ong T, Nammalwar S, Ortuno AI, Meaney DF, Bass CR, Morrison B. Primary blast exposure increases hippocampal vulnerability to subsequent exposure reducing long-term potentiation. J Neurotrauma. 2015

Elder GA, Gama Sosa MA, De Gasperi R, Stone JR, Dickstein DL, Haghighi F, Hof PR, Ahlers ST. Vascular and inflammatory factors in the pathophysiology of blast-induced brain injury. Front Neurol. 2015; 6:48. [PubMed: 25852632]

Goldstein LE, Fisher AM, Tagge CA, Zhang XL, Velisek L, Sullivan JA, Upreti C, Kracht JM, Ericsson M, Wojnarowicz MW, Goletiani CJ, Maglakelidze GM, Casey N, Moncaster JA, Minaeva O, Moir RD, Nowinski CJ, Stern RA, Cantu RC, Geiling J, Blusztajn JK, Wolozin BL, Ikezu T, Stein TD, Budson AE, Kowall NW, Chargin D, Sharon A, Saman S, Hall GF, Moss WC, Cleveland RO, Tanzi RE, Stanton PK, McKee AC. Chronic traumatic encephalopathy in blast-exposed military veterans and a blast neurotrauma mouse model. Sci Transl Med. 2012; 4:134ra160.

Gullotti DM, Beamer M, Panzer MB, Chen YC, Patel TP, Yu A, Jaumard N, Winkelstein B, Bass CR, Morrison B, Meaney DF. Significant head accelerations can influence immediate neurological impairments in a murine model of blast-induced traumatic brain injury. J Biomech Eng. 2014; 136:091004. [PubMed: 24950710]

Heldt SA, Elberger AJ, Deng Y, Guley NH, Del Mar N, Rogers J, Choi GW, Ferrell J, Rex TS, Honig MG, Reiner A. A novel closed-head model of mild traumatic brain injury caused by primary overpressure blast to the cranium produces sustained emotional deficits in mice. Front Neurol. 2014; 5:2. [PubMed: 24478749]

Heltemes KJ, Holbrook TL, Macgregor AJ, Galarneau MR. Blast-related mild traumatic brain injury is associated with a decline in self-rated health amongst US military personnel. Injury. 2012; 43:1990–1995. [PubMed: 21855064]

Hoge CW, McGurk D, Thomas JL, Cox AL, Engel CC, Castro CA. Mild traumatic brain injury in U.S. soldiers returning from Iraq. N Engl J Med. 2008; 358:453–463. [PubMed: 18234750]

Howard AL, Neu A, Morgan RJ, Echegoyen JC, Soltesz I. Opposing modifications in intrinsic currents and synaptic inputs in post-traumatic mossy cells: evidence for single-cell homeostasis in a hyperexcitable network. J Neurophysiol. 2007; 97:2394–2409. [PubMed: 16943315]

Huang MX, Nichols S, Baker DG, Robb A, Angeles A, Yurgil KA, Drake A, Levy M, Song T, McLay R, Theilmann RJ, Diwakar M, Risbrough VB, Ji Z, Huang CW, Chang DG, Harrington DL, Muzzatti L, Canive JM, Christopher Edgar J, Chen YH, Lee RR. Single-subject-based whole-brain MEG slow-wave imaging approach for detecting abnormality in patients with mild traumatic brain injury. Neuroimage Clin. 2014; 5:109–119. [PubMed: 25009772]

Huber BR, Meabon JS, Martin TJ, Mourad PD, Bennett R, Kraemer BC, Cernak I, Petrie EC, Emery MJ, Swenson ER, Mayer C, Mehic E, Peskind ER, Cook DG. Blast exposure causes early and persistent aberrant phospho- and cleavedtau expression in a murine model of mild blast-induced traumatic brain injury. J Alzheimers Dis. 2013; 37:309–323. [PubMed: 23948882]

Hue CD, Cao S, Haider SF, Vo KV, Effgen GB, Vogel E 3rd, Panzer MB, Bass CR, Meaney DF, Morrison B 3rd. Blood-brain barrier dysfunction after primary blast injury in vitro. J Neurotrauma. 2013; 30:1652–1663. [PubMed: 23581482]

Hue CD, Cao S, Dale Bass CR, Meaney DF, Morrison B 3rd. Repeated primary blast injury causes delayed recovery, but not additive disruption, in an in vitro blood-brain barrier model. J Neurotrauma. 2014; 31:951–960. [PubMed: 24372353]

Hue CD, Cho FS, Cao S, Nicholls RE, Vogel EW Iii, Sibindi C, Arancio O, Dale Bass CR, Meaney DF, Morrison B Iii. Time course and size of blood-brain barrier opening in a mouse model of blast-induced traumatic brain injury. J Neurotrauma. 2015

Hunt RF, Scheff SW, Smith BN. Synaptic reorganization of inhibitory hilar interneuron circuitry after traumatic brain injury in mice. J Neurosci. 2011; 31:6880–6890. [PubMed: 21543618]

Jean A, Nyein MK, Zheng JQ, Moore DF, Joannopoulos JD, Radovitzky R. An animal-to-human scaling law for blast-induced traumatic brain injury risk assessment. Proc Natl Acad Sci U S A. 2014; 111:15310–15315. [PubMed: 25267617]

Johnson BN, Palmer CP, Bourgeois EB, Elkind JA, Putnam BJ, Cohen AS. Augmented inhibition from cannabinoid-sensitive interneurons diminishes CA1 output after traumatic brain injury. Front Cell Neurosci. 2014; 8:435. [PubMed: 25565968]

Johnstone VP, Yan EB, Alwis DS, Rajan R. Cortical hypoexcitation defines neuronal responses in the immediate aftermath of traumatic brain injury. PLoS One. 2013; 8:e63454. [PubMed: 23667624]

Kabu S, Jaffer H, Petro M, Dudzinski D, Stewart D, Courtney A, Courtney M, Labhasetwar V. Blast-associated shock waves result in increased brain vascular leakage and elevated ROS levels in a rat model of traumatic brain injury. PLoS One. 2015; 10:e0127971. [PubMed: 26024446]

Kovacs SK, Leonessa F, Ling GS. Blast TBI models, neuropathology, and implications for seizure risk. Front Neurol. 2014; 5:47. [PubMed: 24782820]

Meaney DF, Morrison B, Dale Bass C. The mechanics of traumatic brain injury: a review of what we know and what we need to know for reducing its societal burden. J Biomech Eng. 2014; 136:021008. [PubMed: 24384610]

Nakagawa A, Fujimura M, Kato K, Okuyama H, Hashimoto T, Takayama K, Tominaga T. Shock wave-induced brain injury in rat: novel traumatic brain injury animal model. Acta Neurochir Suppl. 2008; 102:421–424. [PubMed: 19388359]

Ning YL, Yang N, Chen X, Xiong RP, Zhang XZ, Li P, Zhao Y, Chen XY, Liu P, Peng Y, Wang ZG, Chen JF, Zhou YG. Adenosine A2A receptor deficiency alleviates blast-induced cognitive dysfunction. J Cereb Blood Flow Metab. 2013; 33:1789–1798. [PubMed: 23921902]

Ortinski PI, Dong J, Mungenast A, Yue C, Takano H, Watson DJ, Haydon PG, Coulter DA. Selective induction of astrocytic gliosis generates deficits in neuronal inhibition. Nat Neurosci. 2010; 13:584–591. [PubMed: 20418874]

Panzer MB, Matthews KA, Yu AW, Morrison B 3rd, Meaney DF, Bass CR. A multiscale approach to blast neurotrauma modeling: part I - development of novel test devices for in vivo and in vitro blast injury models. Front Neurol. 2012; 3:46. [PubMed: 22470367]

Panzer MB, Wood GW, Bass CR. Scaling in neurotrauma: how do we apply animal experiments to people? Exp Neurol. 2014; 261:120–126. [PubMed: 25035134]

Patel TP, Gullotti DM, Hernandez P, O'Brien WT, Capehart BP, Morrison B 3rd, Bass C, Eberwine JE, Abel T, Meaney DF. An open-source toolbox for automated phenotyping of mice in behavioral tasks. Front Behav Neurosci. 2014a; 8:349. [PubMed: 25339878]

Patel TP, Ventre SC, Geddes-Klein D, Singh PK, Meaney DF. Single-neuron NMDA receptor phenotype influences neuronal rewiring and reintegration following traumatic injury. J Neurosci. 2014b; 34:4200–4213. [PubMed: 24647941]

Rafaels K, Bass CR, Salzar RS, Panzer MB, Woods W, Feldman S, Cummings T, Capehart B. Survival risk assessment for primary blast exposures to the head. J Neurotrauma. 2011; 28:2319–2328. [PubMed: 21463161]

Readnower RD, Chavko M, Adeeb S, Conroy MD, Pauly JR, McCarron RM, Sullivan PG. Increase in blood-brain barrier permeability, oxidative stress, and activated microglia in a rat model of blast-induced traumatic brain injury. J Neurosci Res. 2010; 88:3530–3539. [PubMed: 20882564]

Rosenfeld JV, McFarlane AC, Bragge P, Armonda RA, Grimes JB, Ling GS. Blast-related traumatic brain injury. Lancet Neurol. 2013; 12:882–893. [PubMed: 23884075]

Rowson S, Duma SM. Brain injury prediction: assessing the combined probability of concussion using linear and rotational head acceleration. Ann Biomed Eng. 2013; 41:873–882. [PubMed: 23299827]

Rubovitch V, Ten-Bosch M, Zohar O, Harrison CR, Tempel-Brami C, Stein E, Hoffer BJ, Balaban CD, Schreiber S, Chiu WT, Pick CG. A mouse model of blast-induced mild traumatic brain injury. Exp Neurol. 2011; 232:280–289. [PubMed: 21946269]

Sajja VS, Hubbard WB, Hall CS, Ghoddoussi F, Galloway MP, VandeVord PJ. Enduring deficits in memory and neuronal pathology after blast-induced traumatic brain injury. Sci Rep. 2015; 5:15075. [PubMed: 26537106]

Santhakumar V, Bender R, Frotscher M, Ross ST, Hollrigel GS, Toth Z, Soltesz I. Granule cell hyperexcitability in the early post-traumatic rat dentate gyrus: the 'irritable mossy cell' hypothesis. J Physiol. 2000; 524(Pt 1):117–134. [PubMed: 10747187]

Schwab KA, Ivins B, Cramer G, Johnson W, Sluss-Tiller M, Kiley K, Lux W, Warden D. Screening for traumatic brain injury in troops returning from deployment in Afghanistan and Iraq: initial investigation of the usefulness of a short screening tool for traumatic brain injury. J Head Trauma Rehabil. 2007; 22:377–389. [PubMed: 18025970]

Schwarzbach E, Bonislawski DP, Xiong G, Cohen AS. Mechanisms underlying the inability to induce area CA1 LTP in the mouse after traumatic brain injury. Hippocampus. 2006; 16:541–550. [PubMed: 16634077]

Shetty AK, Mishra V, Kodali M, Hattiangady B. Blood brain barrier dysfunction and delayed neurological deficits in mild traumatic brain injury induced by blast shock waves. Front Cell Neurosci. 2014; 8:232. [PubMed: 25165433]

Smith DH, Hicks RR, Johnson VE, Bergstrom DA, Cummings DM, Noble LJ, Hovda D, Whalen M, Ahlers ST, LaPlaca M, Tortella FC, Duhaime AC, Dixon CE. Pre-clinical traumatic brain injury common data elements: toward a common language across laboratories. J Neurotrauma. 2015; 32:1725–1735. [PubMed: 26058402]

Sundaramurthy A, Alai A, Ganpule S, Holmberg A, Plougonven E, Chandra N. Blast-induced biomechanical loading of the rat: an experimental and anatomically accurate computational blast injury model. J Neurotrauma. 2012; 29:2352–2364. [PubMed: 22620716]

Svetlov SI, Prima V, Kirk DR, Gutierrez H, Curley KC, Hayes RL, Wang KK. Morphologic and biochemical characterization of brain injury in a model of controlled blast overpressure exposure. J Trauma. 2010; 69:795–804. [PubMed: 20215974]

Tate CM, Wang KK, Eonta S, Zhang Y, Carr W, Tortella FC, Hayes RL, Kamimori GH. Serum brain biomarker level, neurocognitive performance, and self-reported symptom changes in soldiers repeatedly exposed to low-level blast: a breacher pilot study. J Neurotrauma. 2013; 30:1620–1630. [PubMed: 23687938]

Terrio H, Brenner LA, Ivins BJ, Cho JM, Helmick K, Schwab K, Scally K, Bretthauer R, Warden D. Traumatic brain injury screening: preliminary findings in a US Army Brigade Combat Team. J Head Trauma Rehabil. 2009; 24:14–23. [PubMed: 19158592]

Tompkins P, Tesiram Y, Lerner M, Gonzalez LP, Lightfoot S, Rabb CH, Brackett DJ. Brain injury: neuro-inflammation, cognitive deficit, and magnetic resonance imaging in a model of blast induced traumatic brain injury. J Neurotrauma. 2013; 30:1888–1897. [PubMed: 23777197]

Tweedie D, Rachmany L, Rubovitch V, Zhang Y, Becker KG, Perez E, Hoffer BJ, Pick CG, Greig NH. Changes in mouse cognition and hippocampal gene expression observed in a mild physical- and blast-traumatic brain injury. Neurobiol Dis. 2013; 54:1–11. [PubMed: 23454194]

Vogel EW III, Effgen GB, Patel TP, Meaney DF, Bass CR, Morrison B Iii. Isolated primary blast inhibits long-term potentiation in organotypic hippocampal slice cultures. J Neurotrauma. 2015

Wall PL. Posttraumatic stress disorder and traumatic brain injury in current military populations: a critical analysis. J Am Psychiatr Nurses Assoc. 2012; 18:278–298. [PubMed: 23053745]

Witgen BM, Lifshitz J, Smith ML, Schwarzbach E, Liang SL, Grady MS, Cohen AS. Regional hippocampal alteration associated with cognitive deficit following experimental brain injury: a systems, network and cellular evaluation. Neuroscience. 2005; 133:1–15. [PubMed: 15893627]

Xie K, Kuang H, Tsien JZ. Mild blast events alter anxiety, memory, and neural activity patterns in the anterior cingulate cortex. PLoS One. 2013; 8:e64907. [PubMed: 23741416]

Yang L, Benardo LS, Valsamis H, Ling DS. Acute injury to superficial cortex leads to a decrease in synaptic inhibition and increase in excitation in neocortical layer V pyramidal cells. J Neurophysiol. 2007; 97:178–187. [PubMed: 16987927]

Yeoh S, Bell ED, Monson KL. Distribution of blood-brain barrier disruption in primary blast injury. Ann Biomed Eng. 2013; 41:2206–2214. [PubMed: 23568152]

Yin TC, Britt JK, De Jesus-Cortes H, Lu Y, Genova RM, Khan MZ, Voorhees JR, Shao J, Katzman AC, Huntington PJ, Wassink C, McDaniel L, Newell EA, Dutca LM, Naidoo J, Cui H, Bassuk AG, Harper MM, McKnight SL, Ready JM, Pieper AA. P7C3 neuroprotective chemicals block axonal degeneration and preserve function after traumatic brain injury. Cell Rep. 2014; 8:1731–1740. [PubMed: 25220467]

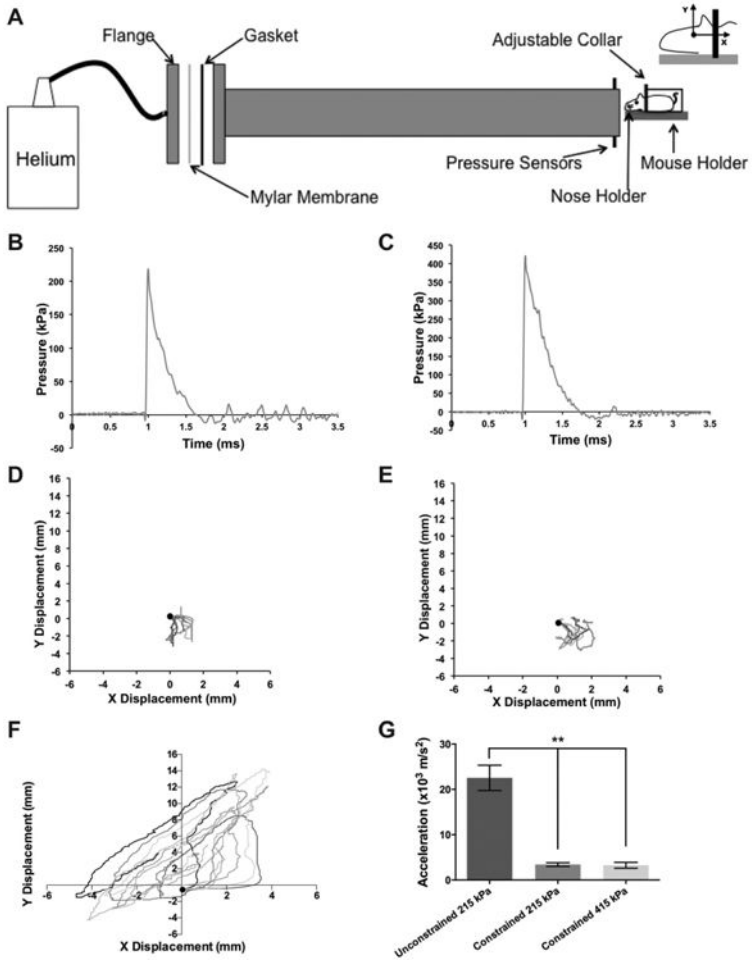

Fig. 1.

Constraining the head significantly reduces the acceleration experienced by it upon impact. (A) Schematic of the shock tube configuration used to create the blast wave exposure. The animal was placed 1 cm outside the exit end of the shock tube in a protective body holder with its head either constrained or unconstrained. (B, C) Representative shockwaves for mild blast (215 kPa peak overpressure) and moderate blast (415 kPa peak overpressure) loading. (D, E) Constraining the head minimizes its displacement during both mild (D) and moderate (E) blast loading. (F) Displacement of the head when it is unconstrained ($n = 13$) during mild blast loading. Exposure to moderate blast loading in this kinematic condition was lethal. (G) The acceleration is significantly larger than when the head is unconstrained under the same loading condition ($p < 0.0001$, Student's *t*-test). There was no significant difference in the accelerations produced by mild ($n = 8$) and moderate ($n = 5$) blast loading ($p = 0.97$; Student's *t*-test).

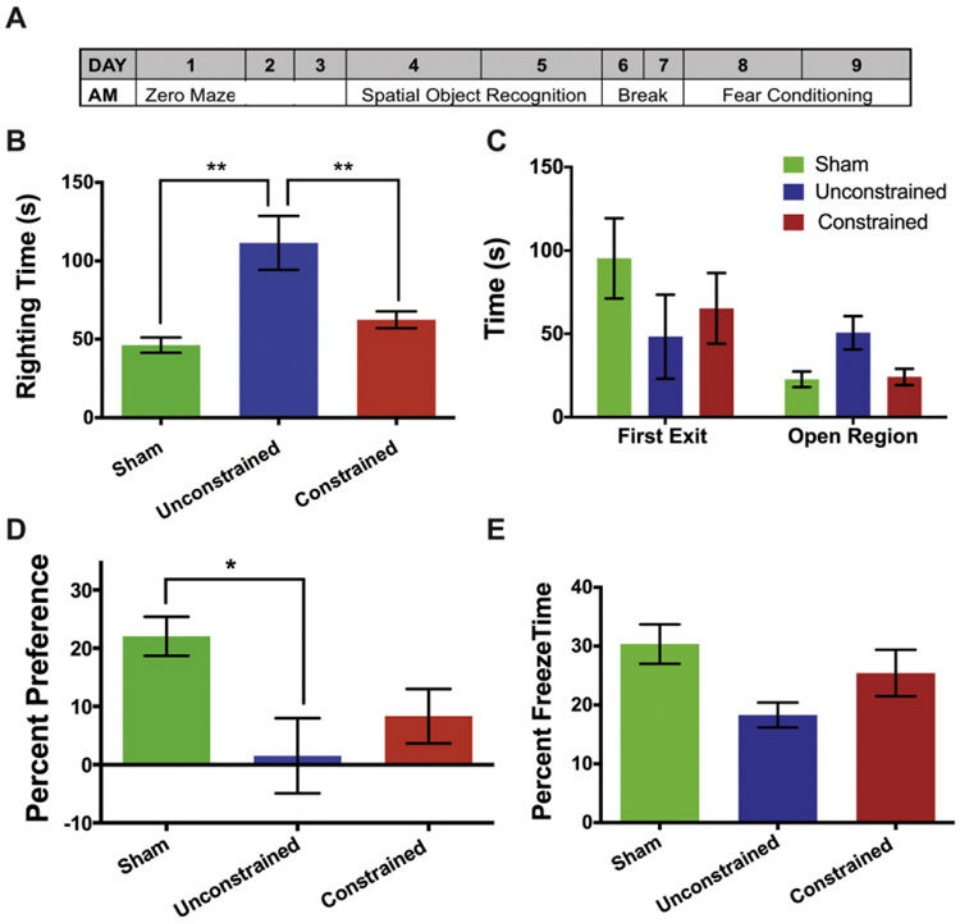

Fig. 2.

Constraining the head resulted in differential changes in some behaviors and not others, subsequent to mild blast loading (215 ± 13 kPa peak overpressure; 46 ± kPa * ms impulse). (A) Time-line of behavioral test battery. (B) Righting time was significantly longer in the unconstrained group ($n = 13$) compared with both sham ($n = 21$) and the constrained (n = 21) group ($p < 0.001$, one-way ANOVA, Tukey's post-hoc). Although righting time was slightly elevated in the constrained group relative to sham, this was not statistically different from sham. (C) Performance measures in an elevated zero-maze. There was no significant difference in the time to first exit the walled portions ($p = 0.16$, Kruskal-Wallis). The unconstrained animals ($n = 13$) spent more time in the open region than the constrained ($n = 21$) and sham ($n = 21$) animals. However, the difference was not significant ($p > 0.05$, Kruskal-Wallis, Dunn's posthoc). (D) Both the constrained ($n = 21$) and unconstrained ($n = 13$) animals showed a decreased preference for the displaced object compared with sham ($n = 21$) in the spatial object recognition task ($p = 0.01$, one-way ANOVA, Tukey's posthoc). However, there was no significant difference in the measure between the two kinematic conditions. (E) The unconstrained animals ($n = 13$) exhibited less freezing behavior compared with sham ($n = 21$) animals. However, the performance of the constrained ($n = 21$) animals was not significantly different from sham animals ($p = 0.05$, Kruskal-Wallis, Dunn's posthoc). * $p < 0.05$ posthoc in all.

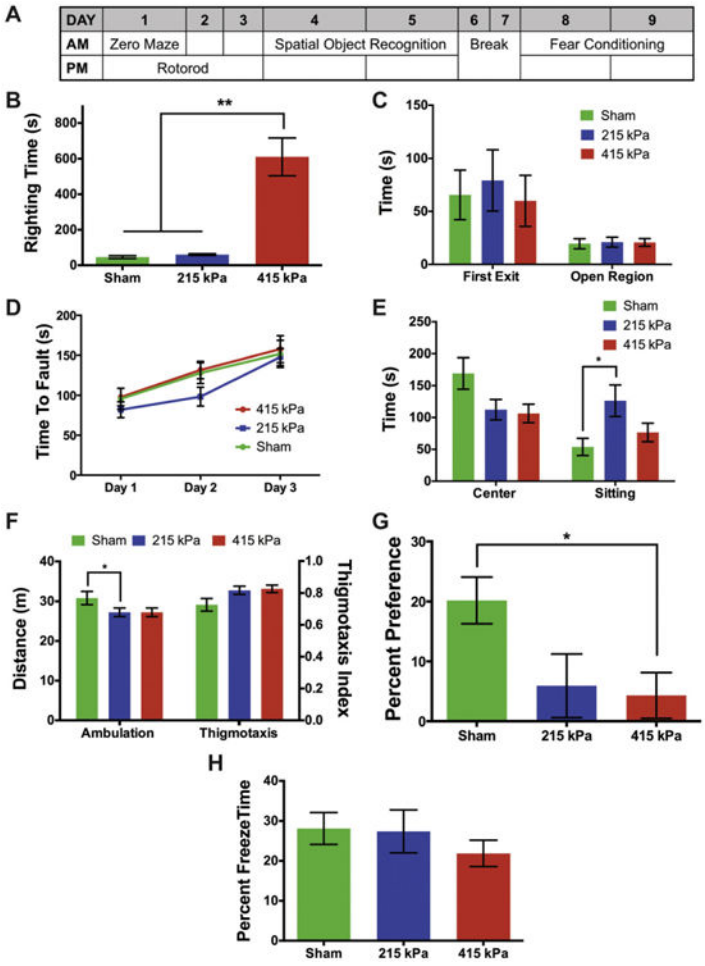

Fig. 3.

Blast loading with constrained head motion caused consistent and similar deficits across two blast exposure levels: mild (215 ± 13 kPa peak; 46 ± kPa * ms impulse) and moderate (415 ± 41 kPa peak; 148 ± 12 kPa * msimpulse). (A) Time-line of behavioral test battery. (B) Righting time for animals exposed to 415 kPa peak overpressure ($n = 12$) were significantly longer compared with those exposed to 215 kPa ($n = 12$) and sham ($n = 12$; $p < 0.001$, one-way ANOVA, Tukey's posthoc). (C) Performance measures in an elevated zero-maze. No significant differences in either measure were observed one day after blast exposure between the three groups ($p = 0.86$ & $p > 0.90$, one-way ANOVA). $n = 12$ animals each in the sham, 215 kPa and 415 kPa groups, respectively. (D) Performance on a rotarod. No significant differences in fault and fall times over three days between the groups ($p = 0.34$, ANOVA). $n = 12$ animals each in the sham, 215 kPa and 415 kPa groups, respectively. (E, F) Measures of open field behavior (day 4). Animals exposed to both levels of blast loading spent significantly less time in the center than the sham ($p = 0.04$, one-way ANOVA, Tukey's posthoc). The total distance traveled (day 4) by both groups of injured animals was significantly lower than in sham animals. ($p = 0.01$, one-way ANOVA, Tukey's posthoc). Both injured groups also showed an increase in thigmotaxis compared with sham ($p = 0.04$, one-way ANOVA, Tukey's posthoc). There was no significant difference in these three measures between the two injured groups. The low exposure group also displayed a

significant increase in sitting behavior relative to sham ($p = 0.02$, one-way ANOVA, Tukey's posthoc). $n = 12$ animals each in the sham, 215 kPa and 415 kPa groups, respectively. (G) Both injured groups showed a decreased preference for the displaced object than sham animals in a SOR task. However, there was no significant difference in the behavior between the two injured groups ($p = 0.02$, one-way ANOVA, Tukey's posthoc). $n = 12$ animals each in the sham, 215 kPa and 415 kPa groups, respectively. (H) There was no significant difference in the fear conditioning response between the three groups ($p = 0.54$, one-way ANOVA). $n = 12$ animals each in the sham, 215 kPa and 415 kPa groups, respectively. *$p <$ 0.05 posthoc in all.

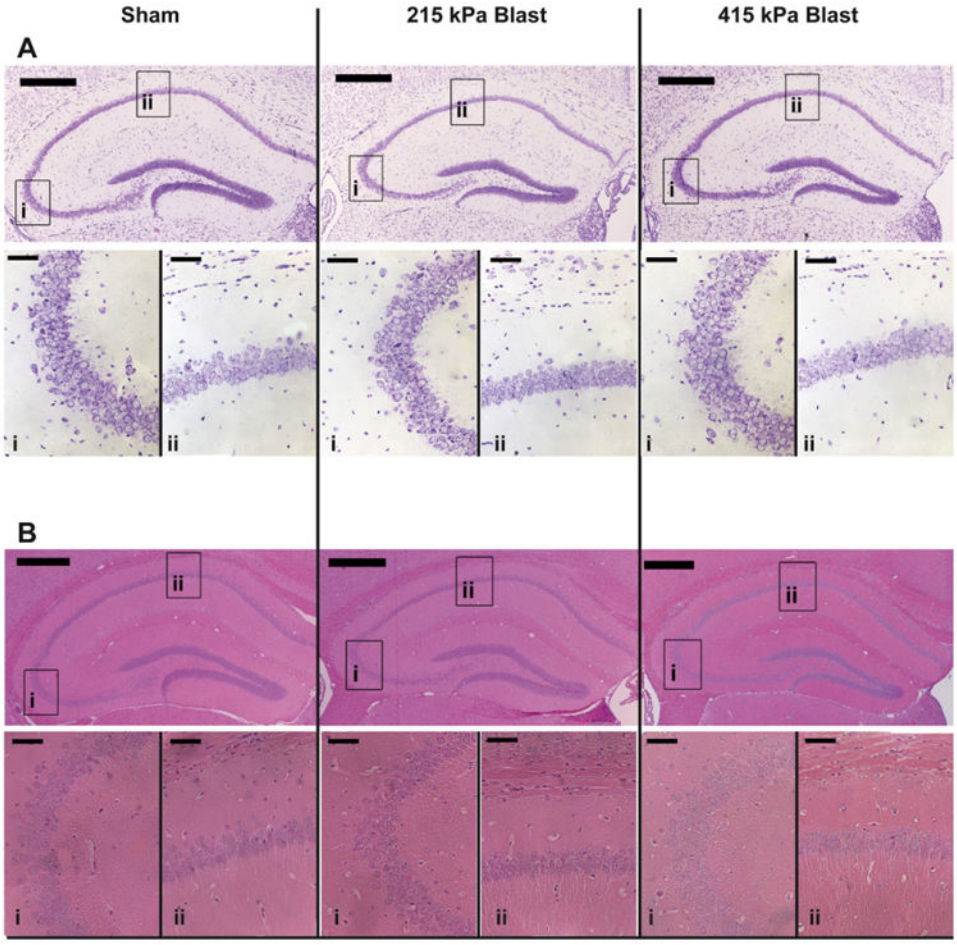

Fig. 4.

Primary blast loading did not reduce neuronal density. Cresyl violet staining (A) and hematoxylin and eosin staining (B) in the hippocampus of sham ($n = 6$) and blast ($n = 7$ in both) exposure groups. There was no significant neuronal loss or evidence for ischemic changes in the three groups. Top panels for each: low magnification (5×) images of the hippocampus. Scale bars: 500 μm. Bottom panels: higher magnification (40×) images of areas CA3 and CA1 (boxes in low magnification images). Scale bars: 50 μm.

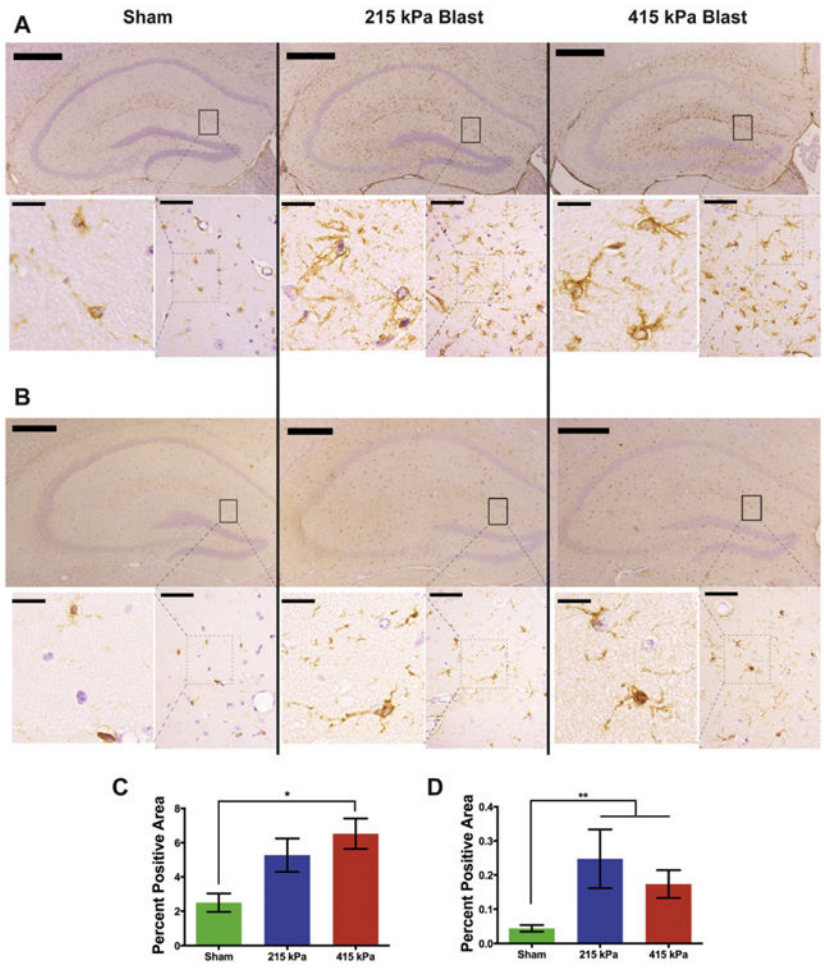

Fig. 5.

Primary blast loading caused reactive astrogliosis in the hippocampus. Staining for GFAP (A, C) and Iba1 (B, D) in the hippocampus increased subsequent to injury (GFAP: $p = 0.01$, Kruskal-Wallis, Dunn's post-hoc; Iba1: $p < 0.01$, Kruskal-Wallis, Dunn's posthoc). However, there was no significant difference in the increase between the two injured groups. $n = 6, 7, 7$ animals in the sham, 215 kPa and 415 kPa groups, respectively. Top panels for each: low magnification (5×) images of the hippocampus. Scale bars: 500 μm. Bottom panels for each (right hand side): higher magnification (63×) images of boxed regions in the low magnification images. Scale bars:50 μm. Bottom panels for each (left hand side): cropped images of the boxed regions in right hand side images. The area of the box is the same in all the images. Scale bars: 50 μm. *$p < 0.05$ posthoc in all.

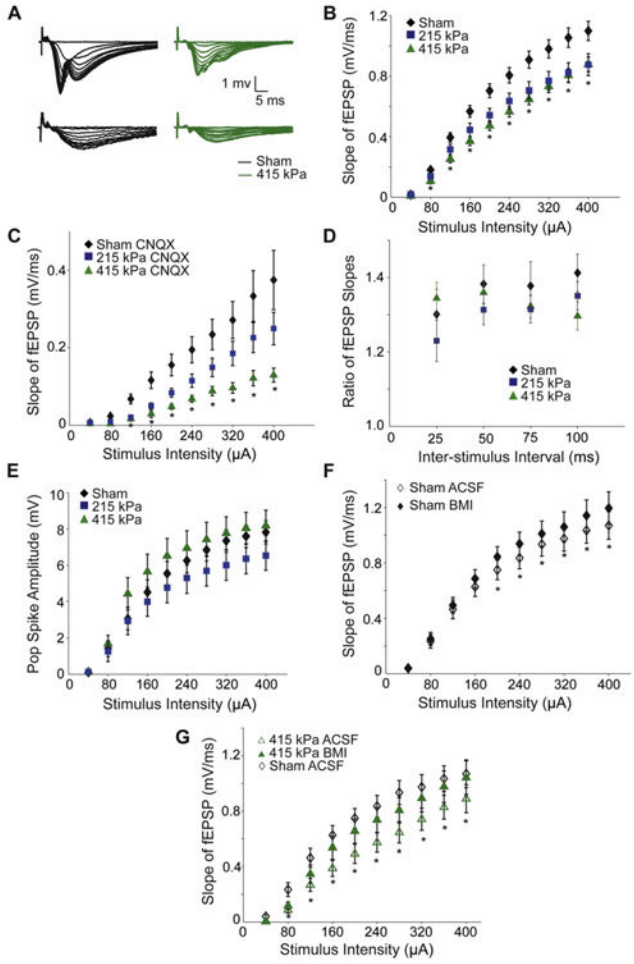

Fig. 6.

Primary blast loading significantly affected hippocampal electrophysiology. (A) Top panel: representative input-output (I/O) curves in stratum radiatum (SR) from slices from sham (black) and moderate blast (green) animals in normal ACSF. Bottom panel: I/O curves from the same slices as in the top panel in mACSF with CNQX. (B) Average slopes of SR field excitatory postsynaptic potential (fEPSP) in slices from sham (n = 40 slices from 16 animals), mild blast (n = 39 slices from 14 animals) and moderate blast (n = 32 slices from 15 animals) animals. There were no significant differences between the two constrained groups for any intensity, but both injured groups were significantly different from sham (p < 0.01, generalized linear model, Waldtest). (C) The slope of the post-CNQX fEPSP was significantly lower at all intensities after moderate blast compared with the post-CNQX slopes in sham (sham, n = 17;215 kPa blast exposure, n = 16; 415 kPa blast exposure, n = 11). The slopes in the mild blast group were significantly smaller at the 80-200 μA stimulus intensities (p < 0.029, one-way ANOVA, Tukey's post-hoc). (D) Paired pulse responses were not significantly different in the three groups (p = 0.21, generalized linear model; sham, n = 29 slices from 13 animals; 215 kPa blast exposure, n = 28 slices from 11 animals; 415 kPa blast exposure blast n = 23 slices from 11 animals). (E) Population spike amplitudes in the three groups (sham, n = 15 slices from 5 animals; 215 kPa blast exposure, n = 14 slices from 5 animals; 415 kPa blast exposure, n = 12 slices from 6 animals). (F) Average slopes of SR

fEPSP in a subset of slices (in B) from sham (14 slices from 7 animals) animals before and after treatment with BMI. *Significantly different, paired *t*-test. (G) Average slopes of SR fEPSP in moderate blast-exposed animals (9 slices from 5 animals) before and after treatment with BMI compared with pre-BMI sham (14 slices from 7 animals) responses. *Pre-treatment responses are significantly different from post-bicuculline (paired *t*-test). There were no significant differences between the post-bicuculline blast responses and the pre- and post-bicuculline sham responses (Student's *t*-test). *$p < 0.05$ posthoc in B, C & E. (For interpretation of the references to color in this figure legend, the reader is referred to the web version of this article.)